ELSEVIER

Biophysical Chemistry 68 (1997) 33–42

Biophysical Chemistry

Structure of Sesbania mosaic virus at 3 Å resolution

M.R.N. Murthy [a,*], M. Bhuvaneswari [a], H.S. Subramanya [a], K. Gopinath [b], H.S. Savithri [b]

[a] *Molecular Biophysics Unit, Indian Institute of Science, Bangalore 560 012, India*
[b] *Department of Biochemistry, Indian Institute of Science, Bangalore 560 012, India*

Received 19 October 1996; revised 2 January 1997; accepted 9 January 1997

Abstract

Sesbania mosaic virus (SMV) is an isometric, ss-RNA plant virus found infecting *Sesbania grandiflora* plants in fields near Tirupathi, South India. The virus particles, which sediment at 116 S at pH 5.5, swell upon treatment with EDTA at pH 7.5 resulting in the reduction of the sedimentation coefficient to 108 S. SMV coat protein amino acid sequence was determined and found to have approximately 60% amino acid sequence identity with that of southern bean mosaic virus (SBMV). The amino terminal 60 residue segment, which contains a number of positively charged residues, is less well conserved between SMV and SBMV when compared to the rest of the sequence. The 3D structure of SMV was determined at 3.0 Å resolution by molecular replacement techniques using SBMV structure as the initial phasing model. The icosahedral asymmetric unit was found to contain four calcium ions occurring in inter subunit interfaces and three protein subunits, designated A, B and C. The conformation of the C subunit appears to be different from those of A and B in several segments of the polypeptide. These observations coupled with structural studies on SMV partially depleted of calcium suggest a plausible mechanism for the initiation of the disassembly of the virus capsid. © 1997 Elsevier Science B.V.

Keywords: Sesbania mosaic virus; Protein structure; X-Ray diffraction; Disassembly

1. Introduction

Small isometric viruses usually have an RNA or DNA genome protected by a protein coat or capsid that is resistant to degradation in the extra cellular environment. A large number of plant and animal viruses have icosahedrally symmetric capsids made of 180 chemically identical protein subunits that encapsidate a single stranded RNA genome of MW 3–4 MDa. Most viruses for which detailed structural studies have been carried out were initially isolated in temperate regions of the world. In contrast, viruses occurring in the tropical regions have not been studied extensively. The emphasis in tropical countries, understandably, has been primarily on epidemiology, host range, geographical distribution, making virus culture and antisera available for diagnosis and identification. In this context, structural studies on tropical viruses is of much interest and will provide information on the diversity in viral architecture and viral evolution. With these objectives, we have determined the amino acid sequence of the coat protein and the three dimensional structure of sesbania mosaic virus (SMV), a plant virus initially isolated from

* Corresponding author.

PII S0301-4622(97)00005-7

Sesbania grandiflora [1,2] occurring in farmers' fields around Tirupathi, Andhra Pradesh, India. SMV is a member of plant sobemovirus group. Three dimensional structure of another sobemovirus, southern bean mosaic virus (SBMV) [3] is known. We have examined the conditions required for the disassembly of virus into protein and RNA and reassembly of virus like particles from isolated components. In this communication, we summarize the results of these investigations and compare the sequence and structure of SMV to other sobemoviruses.

2. Initial studies on SMV

SMV was purified from infected leaves of Sesbania grandiflora plants by differential centrifugation [4]. The virus particles encapsidate a ss-RNA of approximate MW 4 MDa. Purified virus preparations appeared as spherical particles of 300 Å diameter when examined under the electron microscope. The particles had smooth and rounded morphology. Occasional 'empty particles' with dark stain penetrated central regions were observed suggesting that some of the capsids are either devoid of nucleic acid or contain only a fraction of the complete genomic RNA (Fig. 1). The virus moved as a single band in sucrose density gradient centrifugation. The sedimentation coefficient of the virus particles determined by analytical ultracentrifugation was 116 s in 0.05 M Na acetate, pH 5.6 and reduced to 108 s in 0.05 M Tris–HCl, pH 7.5 containing 10 mM EDTA [5]. The coat protein moved as a single band of MW 31 000 in SDS gel electrophoresis [6]. PTA–ELISA [7] and western blotting [8] tests revealed that SMV is serologically related to SBMV and hence belongs to the sobemovirus group of plant viruses [5].

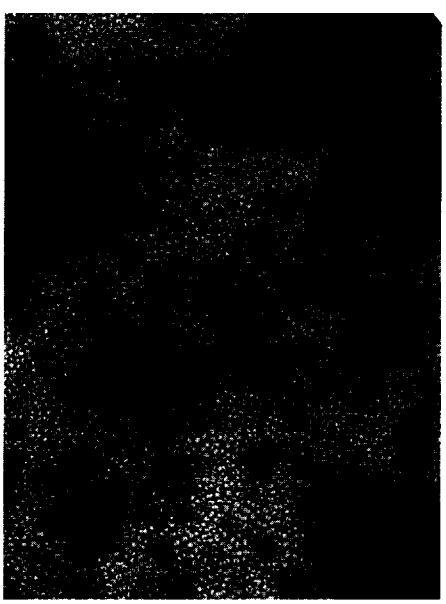

Fig. 1. Electron micrograph of SMV particles stained with 0.1% phosphotungstic acid.

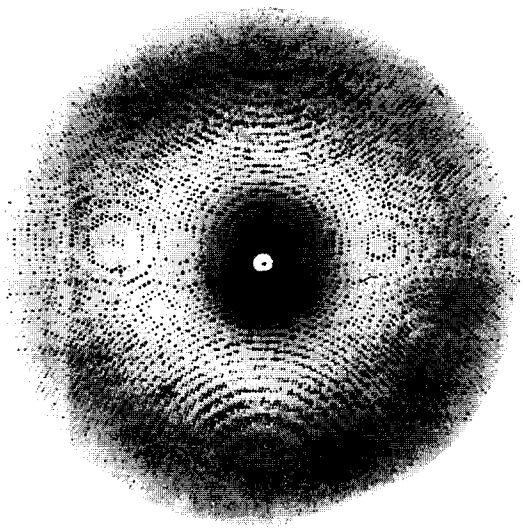

Fig. 2. 0.5° screenless oscillation photograph of a Sesbania mosaic virus crystal. The edge of the photograph corresponds to 2.9 Å resolution. The photograph was recorded by exposing a good crystal to the X-ray beam from an Enraf–Nonius rotating anode generator equipped with a 200 μm focal cup and operating at 40 kV and 40 mA for 40 h.

3. Crystallization of SMV

The purified virus was crystallized for X-ray diffraction studies by vapour diffusion in depression slides [9] using ammonium sulphate as the precipitant. Best crystals were obtained when the virus at a concentration of 30 mg ml^{-1} in 0.1 M sodium acetate, pH 5.6, was precipitated with 15–20% (w/v) ammonium sulphate in the inner well and 30% (w/v) in the outer well. Crystals diffracted to better than 3 Å resolution and belonged to two different forms, although it was difficult to distinguish between them

by observations on external morphology. 2° screenless precession photographs were recorded using one of these crystal forms mounted so as to align the longest axis of the crystal parallel to the spindle. Photographs recorded at spindle settings separated by 72° were superimposable in terms of reflection positions and intensities (data not shown). Oscillation data frames collected using these crystals on a Nicolet–Siemens multiwire detector could not be indexed. These crystals, therefore, might have quasi symmetry. The second crystal form diffracted as well or better (Fig. 2) and belongs to the rhombohedral space group R3 with cell edges of 290 Å and inter axial angles of ca. 62°. The cell edge corresponds to the approximate diameter of the virus particle. The unit cell contains one virus particle and hence the 3-fold axis of the virus particle is along the crystal 3-fold axis.

4. SMV coat protein

The amino acid sequence of the SMV coat protein has been determined [10,4]. Fig. 3 shows alignment of the coat protein sequences of the viruses belonging to the sobemovirus family. The alignment shows that SMV is closer to SBMV-b (bean strain) than SBMV-cp (cowpea strain). There are no changes in the first 53 residues between SBMV-b and SBMV-cp and this corresponds to the most conserved part of the coat protein in these two viruses. SMV on the other hand, has a number of substitutions. The lysine and arginine residues of the amino terminal 65

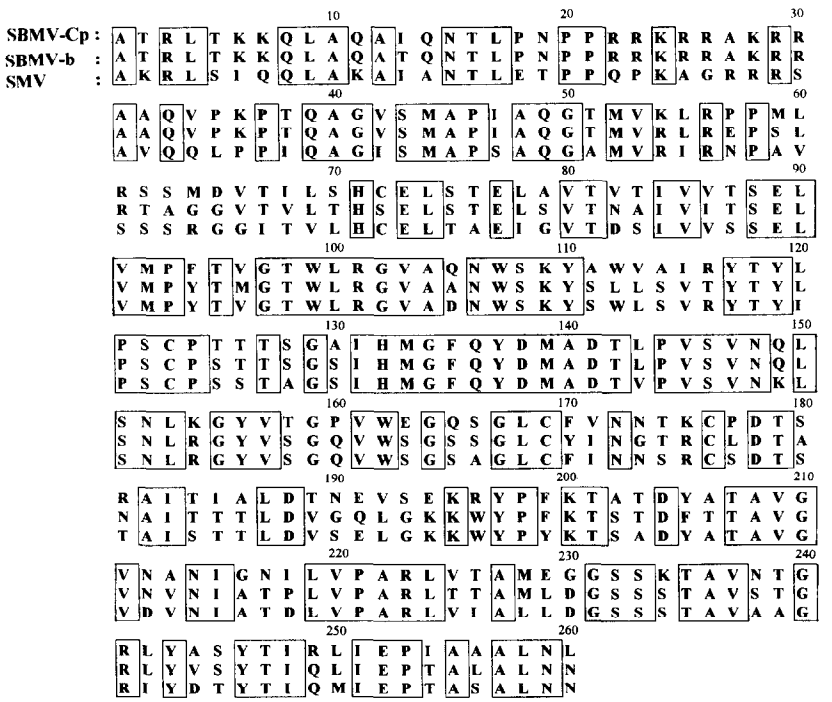

Fig. 3. Comparison of the primary structure of SMV coat protein with that of SBMV cowpea and bean strain viruses. Conserved residues are boxed.

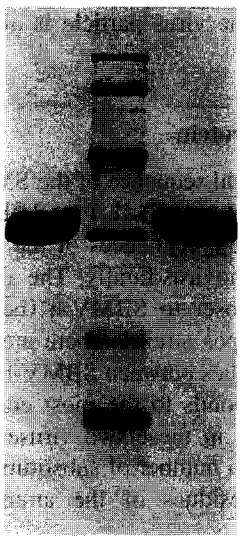

Fig. 4. SDS polyacrylamide gel electrophoresis of SMV coat protein. Lane 1 40 μg of dissociated virus, lane 2 molecular weight markers phosphorylase b (94 kDa), bovine serum albumin (66 kDa), ovalbumin (45 kDa), carbonic anhydrase (30 kDa), soybean trypsin inhibitor (20.5 kDa) and α-lactalbumin (14.4 kDa). Lane 3, SMV coat protein after storage for 48 h at 40 in the absence of RNA.

residues are believed to be important for the assembly of SBMV [11]. These residues also are not well conserved. This suggests that the coulombic forces between protein and nucleic acid are either non-specific or not very important for the assembly of the virus.

The coat protein of SMV can be separated from the genomic RNA by initially incubating the virus (20 mg ml^{-1}) in 0.1 M Tris HCl, pH 7.5, containing 50 mM EDTA followed by precipitation of RNA by the addition of an equal volume of 4 M LiCl. The isolated protein is stable for several days at 4°C (Fig. 4). In contrast, the coat protein of SBMV has been reported to undergo proteolytic degradation under similar conditions [11]. In SBMV, the assembly of protein and nucleic acid into spherical particles is strongly pH dependent [11]. In contrast, SMV protein assembles with SMV RNA at pH 5, 7 and 9 to form particles that are identical to native virus in terms of sedimentation properties (Fig. 5).

5. Collection of X-ray diffraction data on SMV crystals

3D X-ray diffraction data on single crystals of SMV were initially collected on a Nicolet–Siemens area detector [5]. These data were used to establish the icosahedral symmetry of the virus particles, the orientation of the icosahedral symmetry axes with respect to the R3 crystal cell and for demonstrating structural homology between SMV and SBMV [5]. X-ray diffraction data to a higher resolution were subsequently collected by screen less oscillation photography using the multiwire detector and on Kodak DEF-5 films [10]. The area detector frames were processed to 3.5 Å resolution using the XENGEN suite of programs to provide intensities of 203 567 reflections of which 157 134 were independent. Similarly, 410 811 reflection intensities recorded on films were processed to provide intensities of 308 411 independent reflections of which 131 131 corresponded to intensities of partially recorded reflec-

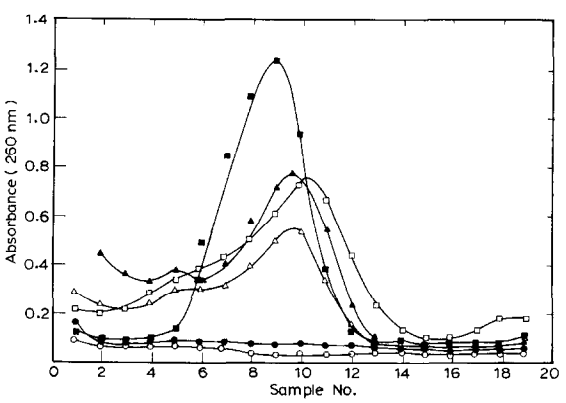

Fig. 5. Sucrose density gradient sedimentation profiles of SMV assembly products. Isolated SMV protein and RNA were mixed in the ratio of 4:1 (w/w) in 0.01 M sodium acetate pH 5, 0.01 M Tris HCl pH 7 or 9 containing 10 mM EDTA. The mixture was dialyzed against the corresponding buffers containing 10 mM $CaCl_2$ instead of EDTA for 24 h and loaded on to 10–40% sucrose gradients containing 10 nM $CaCl_2$ in 0.01 M buffer at the same pH as the reassembly mixture. Centrifugation was carried out for 2 h at 35000 rpm in a SW21 rotor. 0.5 ml fractions were collected manually and monitored for assembly products by recording UV absorbance at 260 nm. SMV coat protein (– ∘ –), SMV RNA (– ∘ –), native virus (– ∘ –) and assembly products, pH 7.5 (– ∘ –), pH 5 (– ∘ –) and pH 9 (– ∘ –). (Reprinted with permission from Gopinath et al. [4]. Copyright by NISCOM, India.).

tions. In the 3.1 to 3.0 Å resolution shell, reflections with $I/\sigma(I) \geq 2.0$ constitute 45% of the theoretically possible reflections. The merging R-factors for the multiwire and film data were 15.8 and 10.9%, respectively ($R = \Sigma(|I_h - \langle I_h \rangle|)/\Sigma I_h \times 100.0$; where I_h is the intensity of reflection h and $\langle I_h \rangle$ is its mean over all the symmetry related measurements). Scaling the multiwire and film data resulted in $R = 8.5\%$ (R defined as $\Sigma|(I_{ad} - I_{film})|/\Sigma(I_{film}) \times 100.0$.

6. SMV structure determination

The three dimensional structure of SMV was determined at 3.0 Å resolution by molecular replacement technique using SBMV as a starting model. Phase refinement by electron density averaging and solvent flattening were carried out to 3.0 Å using a novel procedure which made it possible to carry out all computations to the highest resolution using a computer with 16 MB core memory and 760 MB hard disk. In this procedure, grid positions in the coat protein envelope of the virus were associated with two values: an electron density value and an integer value representing the number of icosahedrally equivalent points which have contributed to the electron density at the reference point. Initially the electron density value and the integer number associated with all grid positions were set to zero. The grid coordinates, associated integer number and electron density values were written as randomly accessible records of 1000 positions. The entire unaveraged map was read in many passes. The numbers associated with grid points in the random access file were updated once for each pass. Starting from the initial electron density map sections, as many sections as could be accommodated in the core memory were read at each pass. For each grid position of the randomly accessible record, the electron density at all points related by non-crystallographic symmetry that fell in the stored map sections were evaluated. The position related by non-crystallographic symmetry are in general non-integral grid points. Electron density at these positions were obtained by linear interpolation using the density values associated with 8 nearest integral grid positions. The interpolated electron density values were summed. The electron density associated with the grid position was incremented by the sum. The associated integer number was incremented by the number of contributing positions. At the end of the last pass containing the terminal sections of the electron density map in core, the integer number associated with all grid positions should be equal to the number of non-crystallographic symmetry (20 in this case) and the value equal to the sum of electron density at the related positions. An averaged map suitable for FFT back transformation was constructed from the random access file.

The initial R-factor for the SBMV model placed in the SMV R3 cell in the orientation revealed by cross rotation function studies was 34% for the 5.5 Å area detector data. The molecular replacement calculations were initiated at 5.5 Å resolution with the area detector data and extended in small steps to 4.5 Å resolution. At this stage, the film data became available. The area detector and the film data sets were scaled together using a locally developed program and the combined data set was used for all subsequent computations. Starting phases as well as phases accepted during extension of resolution were based on a polyalanine model of SBMV. At each stage of refinement, averaging was continued till the

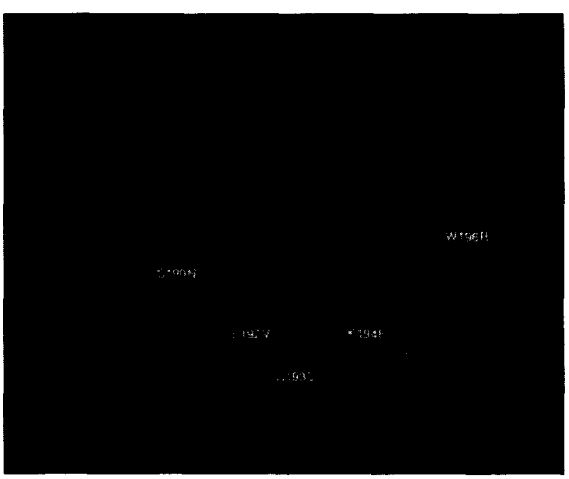

Fig. 6. Map for a small stretch of polypeptide chain illustrating the quality of the final electron density map. The polypeptide in bold represents SMV chain and the light one represents the SBMV-cp. The single letter amino acid code preceding the residue number represents the SMV sequence and the one succeeding represents SBMV-cp sequence.

mean phase change between consecutive cycles was less than a degree. The R-factor and correlation coefficient at the end of molecular replacement calculations were 14% and 0.93, respectively. (R defined as $100 \times \Sigma(|F_0 - F_c|)/\Sigma F_0$ and correlation coefficient as $\Sigma(F_0 - \langle F_0 \rangle)(F_c - \langle F_c \rangle)/(\Sigma(F_0 - \langle F_0 \rangle)^2) \times (\Sigma(F_c - \langle F_c \rangle)^2)^{1/2}$. The final electron density map was used to construct polypeptide models for the A, B and C subunits of the icosahedral asymmetric unit using the program FRODO [12]. The resulting coordinates were refined using the program XPLOR [13]. Strict icosahedral symmetry was imposed on the model. The final refined structure has an R-factor of 22.7% ($R = 100.0 \times \Sigma(F_0 - kF_c)/\Sigma F_0$) with good geometry. The RMS deviations of the bond lengths and angles from standard values are 0.014 Å and 1.77°, respectively. ψ, ϕ values at all Cα carbon atoms are within the allowed regions of the Ramachandran diagram.

7. Subunit structure and organization

The quality of the final electron density map is illustrated in Fig. 6. The three subunits in the icosahedral asymmetric unit (Fig. 7) are designated as A, B and C following the nomenclature used in the description of other $T = 3$ virus structures. 5 A type subunits interact at the icosahedral 5-fold to form pentamers while 3 each of B and C type subunits form hexamers at the icosahedral 3-fold axes. The A, B and C subunits of the icosahedral asymmetric unit are related by an approximate or quasi 3-fold symmetry. There are two distinct type of dimers in the $T = 3$ capsid (Fig. 7). The CC2 dimers are related by an exact icosahedral 2-fold axis while the AB5 dimers are related by a quasi 2-fold axis. The subunit structure consists of an 8-stranded anti-parallel β-barrel (βB-βH, residues 66–260, S-domain) and a 65 residue extension from the S-domain towards the interior of the virus (R-domain, residues 1–65) The subunit structure and their organization are very similar to those of SBMV [3] and several other isometric viral coat proteins. The amino terminal 65 residues are disordered in the A and B subunits. In C subunits, residues 1–38 are disordered while the rest are ordered. Residues 43–53 of the R domains of 3 C type subunits related by icosahedral 3-fold axis

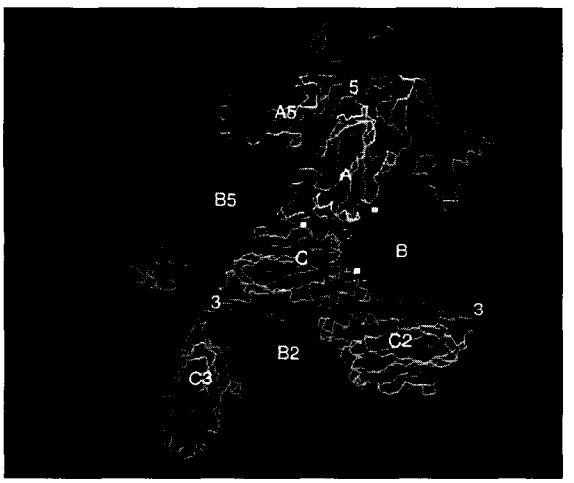

Fig. 7. The icosahedral asymmetric unit of several commonly occurring plant isometric viruses contains 3 protein subunits. The asymmetric unit is a wedge defined by two neighbouring 3- and 5-fold axis as shown. 5 protein subunits cluster around the icosahedral 5-fold and form a pentameric capsomere. 6 subunits cluster around the icosahedral 3-fold axis to form a hexameric capsomere. The icosahedral 3-fold axis is also a quasi 6-fold axis. The nomenclature (A, B or C) used to designate protein subunits is also shown.

form a hydrogen bonded network which has been described as a β annulus structure [14]. It has been proposed that this unique structure might be important for the error free assembly of $T = 3$ capsids [15,16].

8. Refined thermal parameters

The variation of the B-factors of Cα atoms along the polypeptide obtained independently for the A, B and C subunits are shown in Fig. 8. The B-factor distribution for the A, B, C subunits show excellent correlation reflecting the reliability of the refined B values. The B-factors are higher than 20 Å^2 only for the amino terminal and the loop regions that connect secondary structural elements. Although the polypeptide is ordered from residue 39 in the C subunits, residues 62–65 have relatively large B-factors. This flexibility might be significant for the alternate conformations observed for the amino terminal arm. In all the three subunits, the thermal parameters are high around residue 174. This region is completely

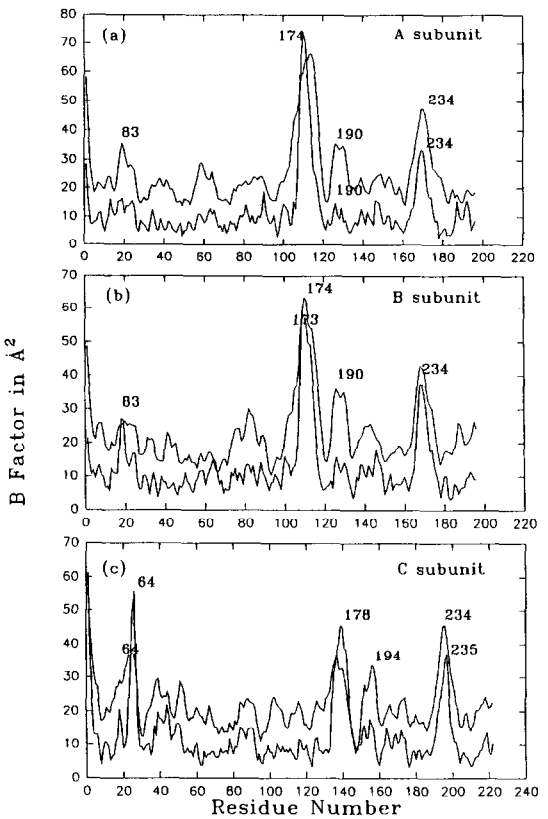

Fig. 8. Variation of refined thermal parameters at the Cα atoms of A, B and C subunits. The lower curve corresponds to B factors of SMV while the upper curve to SBMV.

buried in the virus and is in close proximity with the disordered RNA. Thermal parameters are also consistently high for residues around 235. This corresponds to the loop that is most exposed to the solvent. Fig. 9 illustrates the distribution of thermal parameters with respect to the tertiary fold and quaternary organization of the subunits as a coded diagram. It is apparent that the loops that interact at the icosahedral 5-fold and 3-fold axes have larger B-factors than the rest of the residues. This mobility might be important for packing of chemically identical subunits into quasi-equivalent pentamers and hexamers.

9. Putative calcium binding sites

In addition to the protein subunits, four putative calcium ions have been located in the icosahedral asymmetric unit of SMV. Three of these ions are related by quasi 3-fold symmetry, as in the case of SBMV. These occur at the AB, BC and CA inter subunit interfaces. The positions of these ions are at a distance of 136.7, 131.9 and 135.6 Å from the viral centre, respectively. Five of the ligands emanate from the protein subunits while the sixth ligand is a probable water bound to carbonyl oxygen of Ser108. Of the five ligands to the calcium in the AB subunit interface, three are from the B subunit and the others are from the A subunit. The ligands from the A subunit are carboxylate oxygens from the side chains of Asp138 and Asp141. A twelve residue segment around these residues is the most conserved region in sobemoviruses. Main chain carbonyl oxygens of Tyr199, Asn259 and amide oxygen of Asn257 are the ligands contributed by the B subunit. The chemical environment of the calcium ions in the CB and AC subunit interfaces are indistinguishable except that the ligands emanate from corresponding quasi-equivalent subunits. There is an additional calcium ion in SMV on or near the quasi 3-fold axis. The ligands to this calcium are not easily identified from the electron density map. It is likely that three of the ligands are carboxylates of D218 from the A, B and C subunits.

Systematic studies have been carried out to exam-

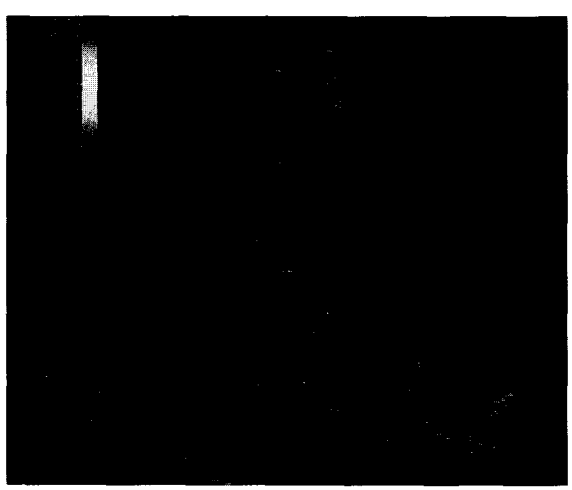

Fig. 9. Refined thermal parameters of the A, B and C subunits displayed as a coded diagram. The loops at the icosahedral 5- and 6-fold axes show larger B-factors.

ine the effect of EDTA treatment on the degree to which calcium ions are removed from different, quasi-equivalent intersubunit interface [10]. Although the ligand binding geometry is nearly identical at AB, AC and BC interfaces, these studies suggest that the calcium at the BC interface is more susceptible to chelating agents although it is more buried when compared to the calcium at the AB and AC interface. Removal of calcium at the BC interface might lead to disruption of the BC and CC2 interactions.

10. Special aspects of C subunit conformation

C subunit, in contrast to A and B subunits has a partially ordered R domain. In addition, C subunit has other significant differences from A and B subunits which become apparent by a careful examination of the deviation at the Cα atoms when pairs of A, B, and C subunits are superposed (Fig. 10). Between the A and B subunits the RMS deviation is 0.47 Å. Large deviations are observed in the comparison of A and C or B and C subunits, where the RMS deviations are 0.60 and 0.77 Å, respectively. There are only two regions that are significantly different between A and B subunits. One of these regions corresponds to the loop around 171–179 which is in close proximity with RNA and shows signs of partial disorder. Further, this loop is involved in AA5 interactions at the icosahedral 5-fold. The quasi equivalent interaction at the icosahedral 3-fold in the hexameric capsomeres is absent. The only other major difference between A and B subunits occurs in the helix around residue 147. This helix is in the pentameric interface in A subunits while it occurs in the hexameric interface in B and C subunits. In contrast to the two localized regions of difference between A and B subunits, a large number of segments appear to have significant differences when C subunits are compared with A or B subunits. These differences in the C subunit structure from those of A and B subunits observed in SMV are also retained in the structure of SBMV. The RMS deviations when the A, B and C subunits of SMV when compared to the corresponding subunits of SBMV are 0.55, 0.57 and 0.44 Å, respectively. Thus, the C subunit structures, in the two related sobemoviruses, are slightly but significantly different from those of A and B subunits.

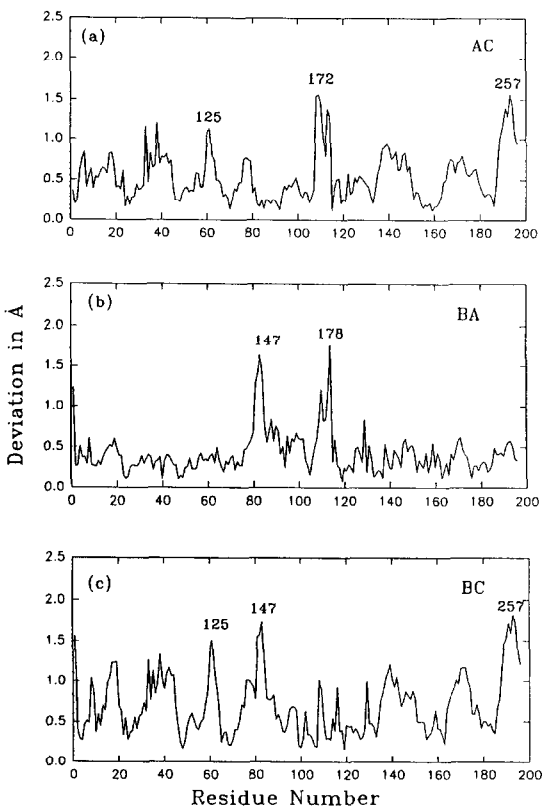

Fig. 10. Residual distances between corresponding Cα positions in the superposition of AB, BC and CA subunits of SMV. (Reprinted with permission from Bhuvaneswari et al. [10]. Copyright Current Biology Ltd., London.)

11. Conclusions

Comparative studies on related viruses provide insights into molecular interactions that are likely to be important for stability and assembly. Comparison of the amino acid sequences of sobemo virus coat proteins clearly establish a divergent evolutionary relationship between SMV, SBMV-cp and SBMV-b. The a priori probability that 53 consecutive residues are identical at the amino terminus of SBMV-b and SBMV-cp, which have 76% amino acid identity in their sequences, is 0.4 in 10 million. Hence, it is highly improbable that the observed identity at the

amino terminus is a result of divergent evolution. This identity, therefore, might represent a rare but interesting case of horizontal transfer of genetic information. The amino terminal region, shown to strongly influence the assembly of isolated protein and nucleic acid in SBMV-cp [11] is not well conserved between SMV and SBMV. Similarly, the positively charged residues of the S-domain also are not conserved to an extent greater than that of the other residues. These observations suggest that electrostatic interactions may not dictate the mode of assembly in these viruses. Although the capsid structures of SMV and SBMV are very similar, partially ordered RNA is seen in SBMV [17] but not in SMV. Similar differences in the degree of order in the RNA structure has been observed in the related structures of CPMV [18] and BPMV [19]. Hence, these interactions are unlikely to exert severe constraints on virus assembly. Two different propositions have been made for the mechanism of assembly in isometric $T = 3$ viruses. Several $T = 3$ virus structures are characterized by the occurrence of the β-annulus structure that links three CC2 dimers at the icosahedral 3-fold axes. Conservation of residues of β annulus suggests that this interaction might be important for assembly. Olson et al. [15] have pointed out the plausible importance of this structure for the error free assembly of $T = 3$ particles. However, the β-annulus is not present in cowpea chlorotic mottle virus [20] and carnation mottle virus [21] although these viral capsids assemble correctly to form $T = 3$ particles. Based on the more numerous molecular interactions between AB dimers when compared to the CC dimers and on the observation that SBMV protein exists as dimers in solution, Rossmann [16] has suggested that the assembly of these viruses might be initiated by the interaction between 5 AB type dimers at the icosahedral 5-fold axis. The results of the present investigation suggest that the final steps of assembly could be the addition of calcium and formation of CC2 and BC interfaces. The chemical context of the calcium ions at the quasi equivalent interfaces are identical. In spite of this, EDTA treatment results in preferential removal of calcium at the BC interface. Removal of calcium at the BC interface might lead to disruption of the interaction between BC and the CC2 interfaces leading to separation of CC2 dimers and AB5 decamers. This might be a first step in the disassembly of the virus.

Acknowledgements

A large number of associates have contributed to the research projects on viruses at Bangalore. We would like to gratefully acknowledge the support and encouragement of S. Munshi, C.N. Hiremath, A. Karande, M.V. Nayudu, S. Suryanarayana, A.N.K. Jacob, N. Ramesh, S. Sundaresh, V. Srividya, C.T. Ranjit Kumar, M. Shastry, J. Joseph G. Lokesh, K. Suguna, M. Vijayan and N. Appaji Rao. Govindaswamy and J. Paul provided technical assistance. The work reviewed here has been generously supported by the Department of Science and Technology and Department of Biotechnology (to MRN and HSS), India.

References

[1] B.S. Solunke, S. Eranna, M.V. Nayudu, Indian Phytopathol. 36 (1983) 568.
[2] P. Sreenivasulu, M.V. Nayudu, Curr. Sci. 51 (1982) 86.
[3] C. Abad-Zapatero, S.S. Abdel-Meguid, J.E. Johnson, A.G.W. Leslie, I. Rayment, M.G. Rossmann, D. Suck, T. Tsukihara, Nature (London) 286 (1980) 33.
[4] K. Gopinath, S. Sundaresh, M. Bhuvaneswari, A. Karande, M.R.N. Murthy, M.V. Nayudu, H.S. Savithri, Indian J. Biochem. Biophys. 31 (1994) 322.
[5] H.S. Subramanya, K. Gopinath, M.V. Nayudu, H.S. Savithri, M.R.N. Murthy J. Mol. Biol. 229 (1994) 20.
[6] U.K. Laemmli, Nature (London) 277 (1970) 680.
[7] W.P. Mowat, S. Dawson, J. Virol. Meth. 15 (1987) 233.
[8] R. Koenig, W. Burgermeister, in: R.A.C. Jones, L. Torrace (Eds.), Developments and Applications in Virus Testing, Assoc. Appl. Biologists, Warwick, UK, 1986, pp. 121–137.
[9] A. McPherson, in: Preparation and Analysis of Protein Crystals, Wiley-Interscience, New York, 1982.
[10] M. Bhuvaneswari, H.S. Subramanya, K. Gopinath, H.S. Savithri, M.V. Nayudu, M.R.N. Murthy, Structure 3 (1995) 1021.
[11] H.S. Savithri, J.W. Erickson, Virology 126 (1983) 328.
[12] T.A. Jones, J. Appl. Cryst. 11 (1992) 268.
[13] A.T. Brunger (1992), X-PLOR Manual, Version 3.1, Yale University, New Haven, CT.
[14] S.C. Harrison, A. Olson, C.E. Schutt, F.K. Winkler, G. Bricogne, Nature (London) 276 (1978) 368.
[15] A.J. Olson, G. Bricogne, S.C. Harrison, J. Mol. Biol. 171 (1983) 61.
[16] M.G. Rossmann, Virology 134 (1984) 1.

[17] A.M. Silva, M.G. Rossmann, J. Mol. Biol. 197 (1987) 69.
[18] C.V. Stauffacher, R. Usha, M. Harrington, T. Schmidt, M.V. Hosur, J.E. Johnson, in: D. Moras, J. Drenth, B. Strandberg, D. Suck, D. Wilson (Eds.), Crystallography and Molecular Biology, Plenum, New York, 1987, p. 293.
[19] Z. Chen, C. Stauffacher, Y. Li, T. Schmidt, W. Bomu, G. Kamer, M. Shanks, U. Lomonossoff, J.E. Johnson, Science 245 (1989) 154.
[20] J.A. Speir, S. Munshi, G. Wang, T.S. Baker, J.E. Johnson, Structure 3 (1995) 63.
[21] E. Yu. Morgunova, Z. Dauter, E. Fry, D.I. Stuart, V.Ya. Stelmaschuk, A.M. Mikhailov, K.S. Wilson, B.K. Vainshtein, FEBS Lett. 338 (1994) 267.